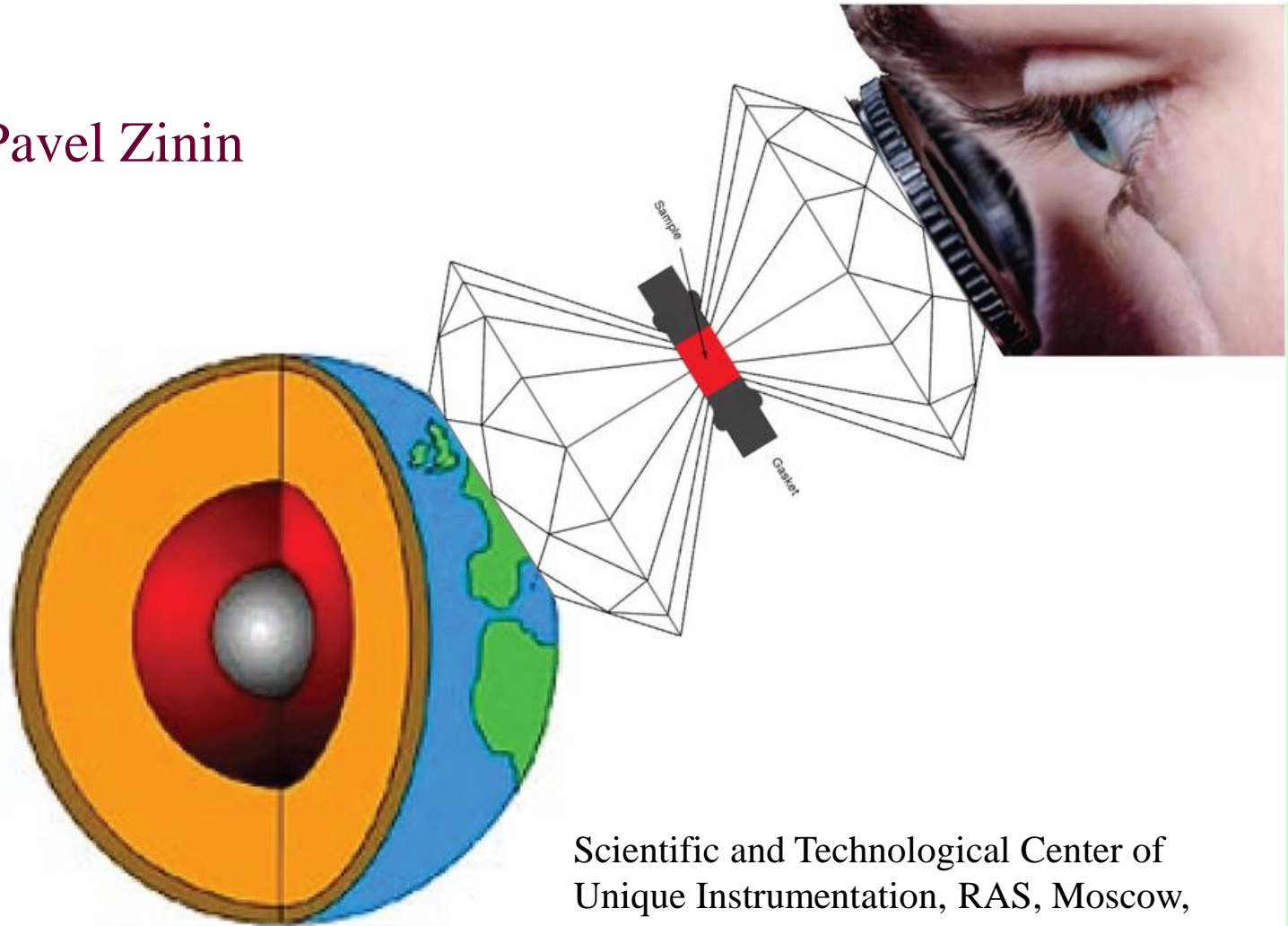


# Elastic properties of minerals and functional materials by Brillouin scattering and laser ultrasonics

Pavel Zinin



Scientific and Technological Center of  
Unique Instrumentation, RAS, Moscow,  
Russia

# Motivation

- Understanding of the elastic behavior of minerals under high pressure is a crucial factor for developing a model of the Earth's structure because most information about the Earth's interior comes from seismological data.

**Birch's law** establishes a linear relation of the compressional wave velocity  $v_p$  of rocks and minerals of a constant average atomic weight  $M_{avg}$  with density as:

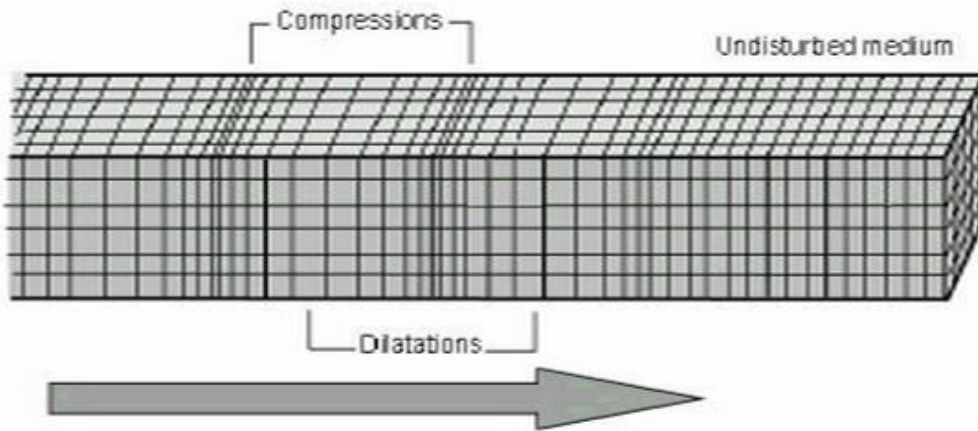
$$v_p = a(M_{avg}) + b\rho$$

for some function  $a(x)$ .

- Laboratory measurements of *velocities and other elastic properties of minerals are the key to understanding this seismic information*, allowing us to translate it into quantities such as chemical composition, mineralogy, temperature, and preferred orientation of minerals.
- We chose to use iron for two reasons: (a) The study of acoustical wave propagation in iron under high pressure has a direct *application in geophysics*. Iron is thought to be the main constituent of the Earth's core (Birch 1952); (b) iron is a material in which acoustical waves are easily excited by a short laser pulse. *Success in acousto-optic* detection of sound waves in iron under high pressure opens the way to study elastic properties of other geological and functional materials. A thin layer of iron can also be used as a transducer for opto-acoustical sound excitation and acousto-optical sound detection in DAC loaded with different non-transparent material.

# P and S waves

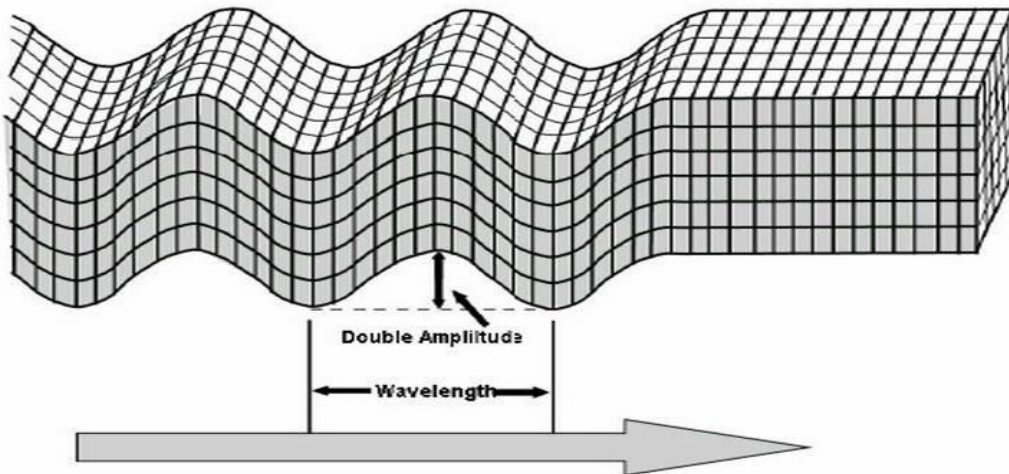
## P Wave



Longitudinal (Compression) Waves - The particles of the medium undergo displacements in a direction parallel to the direction of wave motion.

$$V_P = \sqrt{\frac{K_S + (4/3)\mu}{\rho}}$$

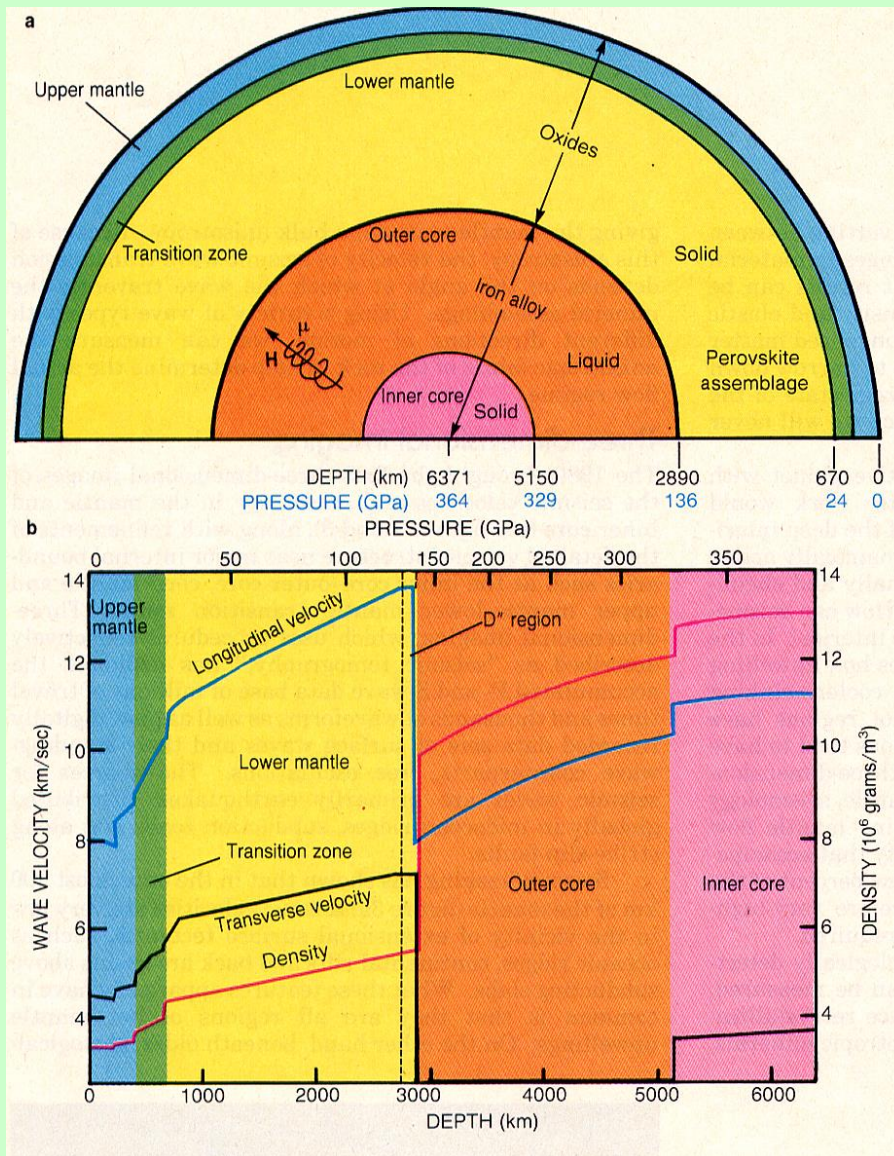
## S Wave



Transverse Waves - The particles of the medium undergo displacements in a direction perpendicular to the wave motion.

$$V_S = \sqrt{\frac{\mu}{\rho}}$$

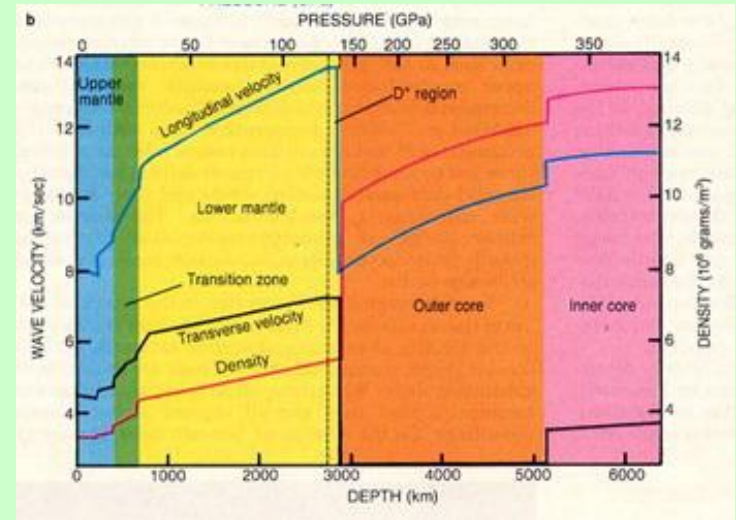
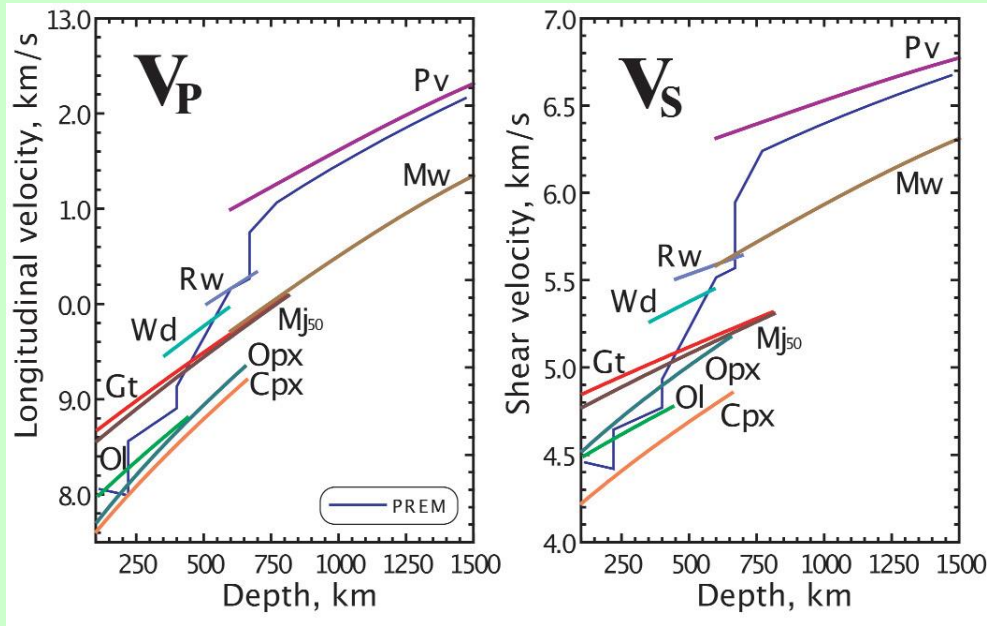
# Cross Sections of the Earth and Its Elastic Properties



Seismological images of the Earth's mantle reveal three distinct changes in velocity structure, at depths of 410, 660 and 2,700 km. The first two are best explained by mineral phase transformations, whereas the third—the D" layer—probably reflects a change in chemical composition and thermal structure.

Average elastic parameters as a function of depth. The P-wave velocity  $V_p$ , S-wave velocity  $V_s$ ; and density  $\rho$  are determined from seismological analysis. The figure is based on the Primary Reference Earth Model (PREM). PREM was created in 1981 (Dziewonski and Anderson, *Phys. Earth. Planet. Int.*, **25**, 297).

# Elastic Properties of Minerals



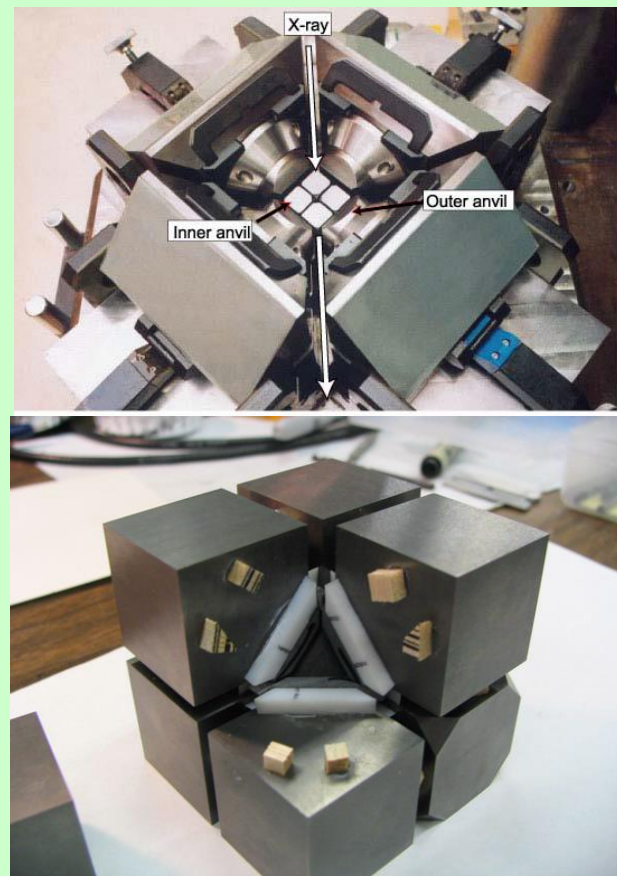
Lay *et al.*, *Physics Today*, 1990

The variation in sound velocity with depth for various key mantle minerals: olivine (Ol), diopside (Cpx), enstatite (Opx), garnet (Gt), majorite-garnet solid solution (Mj<sub>50</sub>), wadsleyite (Wd), ringwoodite (Rw), magnesiowüstite (Mw), Mg-silicate perovskite (Pv). Increases in temperature for an adiabatic gradient are taken into account. The reference model PREM Primary Reference Earth Model (Dziewonski and Anderson 1981) is shown for reference. The length of an adiabat indicates approximately the maximum pressure stability of any given phase. (From Bass, *Elements*, 2008 ).

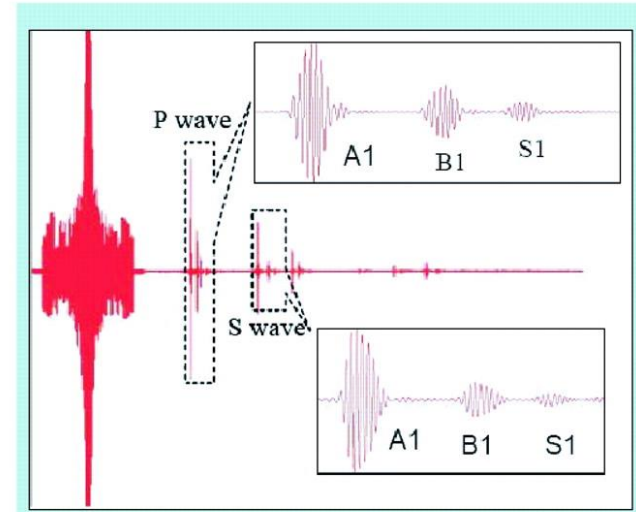
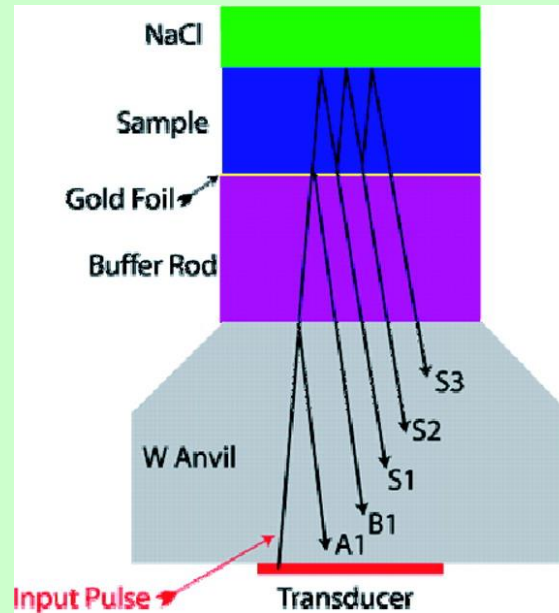
More than fifty years ago, Birch proposed a simple empirical equation, Birch's law, that relates sound velocity to the density and mean atomic weight of the material the sound is passing through.

As pointed out by Bassett, because of this relation the velocity of sound can be measured in the Earth's interior as seismic waves travel from an earthquake on one side of the Earth to a seismograph on the other and can also be measured in the laboratory by sending ultrasound through samples at controlled pressures and temperatures.

# Ultrasound Measurements in Large Volume Press Apparatus



Photos of outer (Top) and inner (Bottom) anvils in LVP

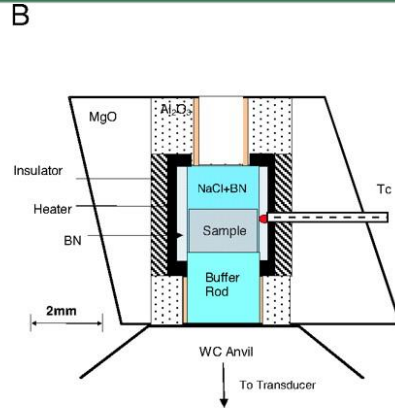
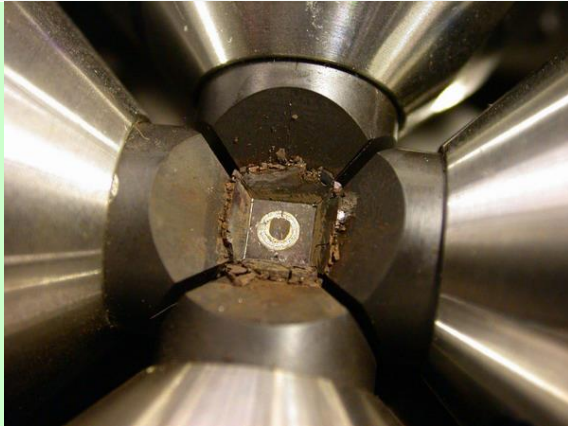


Schematic of acoustic wave propagation in the current experimental configuration for simultaneous measurement of  $P$  and  $S$  wave velocities in multi-anvil high-pressure apparatus (Left) and the acoustic signals generated and received by using acoustical transducer (Right) to allow rapid data collection and off-line analysis (From Li, Liebermann, PNAS, **104**, 9145, 2007).

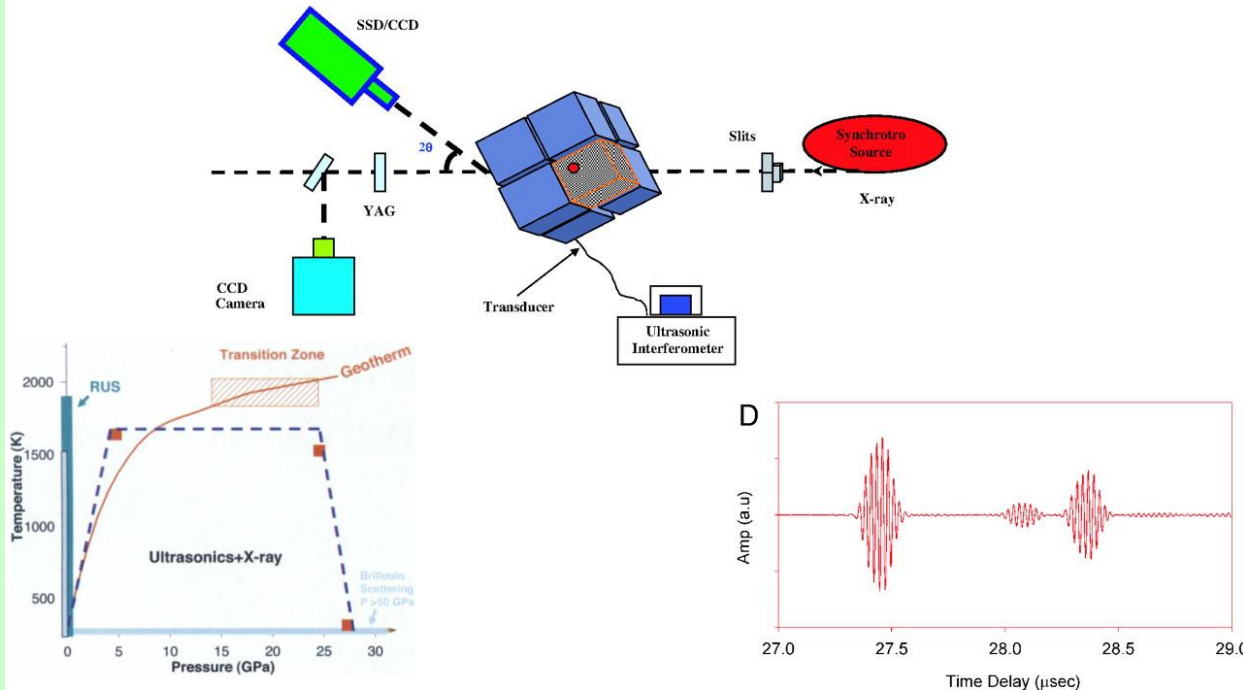
For a cubic crystal under hydrostatic pressure

$$d = \frac{d_o}{s(P)}; ds = \frac{s}{C_{11} + 2C_{12}} dP$$

# Ultrasonic Interferometry Measurements in Conjunction with Synchrotron X-ray Radiation

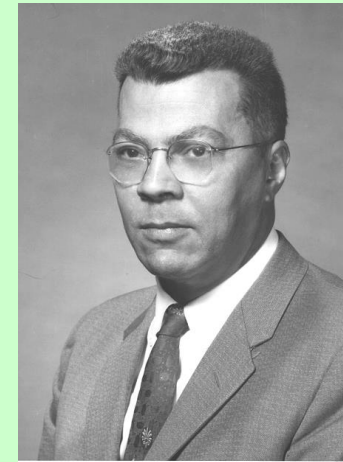
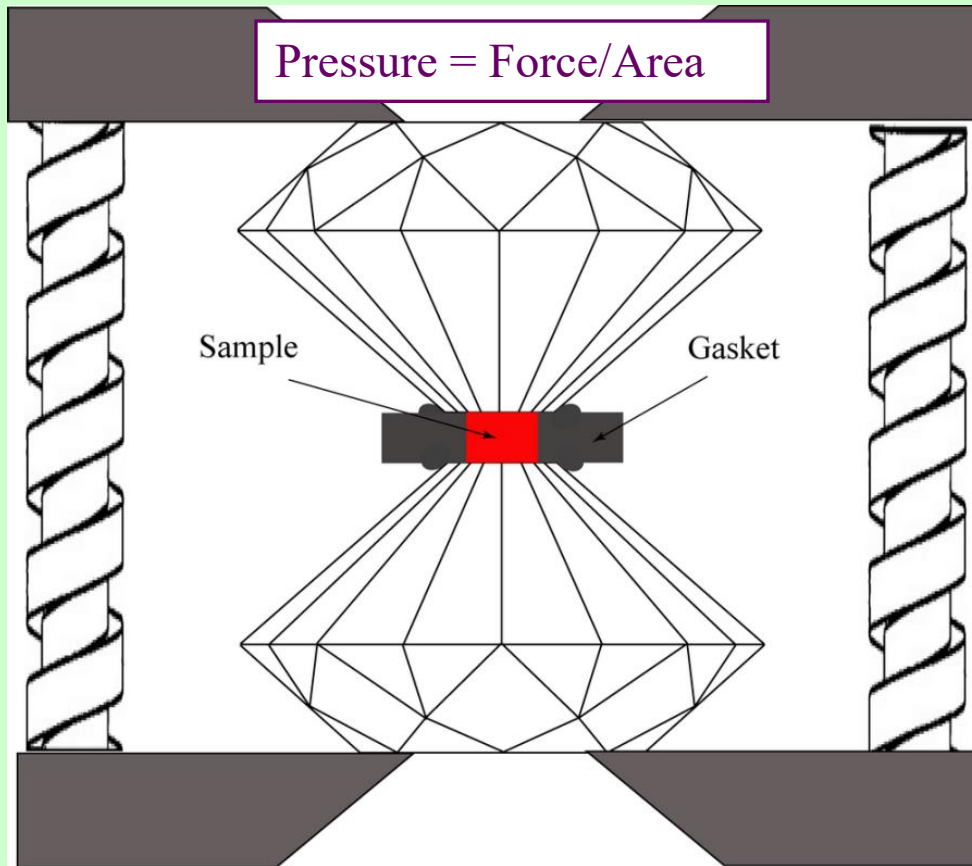


Schematic diagram of experimental configuration for ultrasonic interferometry measurements in conjunction with synchrotron x radiation in the Kawai-type, multi-anvil apparatus at the Advanced Photon Source, Argonne National Laboratory

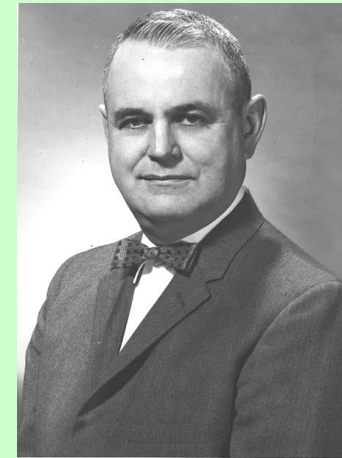


Zhou, et al., Elasticity and sound velocities of polycrystalline  $Mg_3Al_2(SiO_4)_3$  garnet up to 20 GPa and 1700K, *J. Appl. Phys.* 2012.

# Diamond Anvil Cell



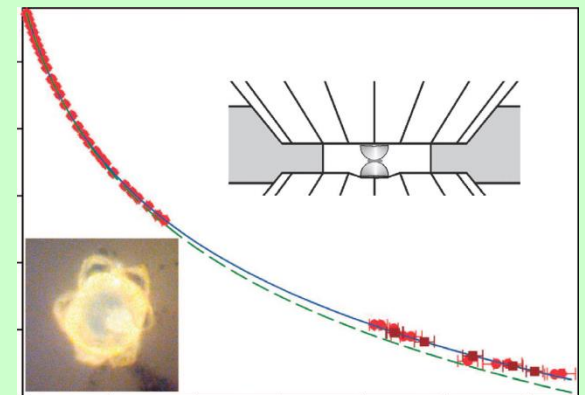
Charles Weir



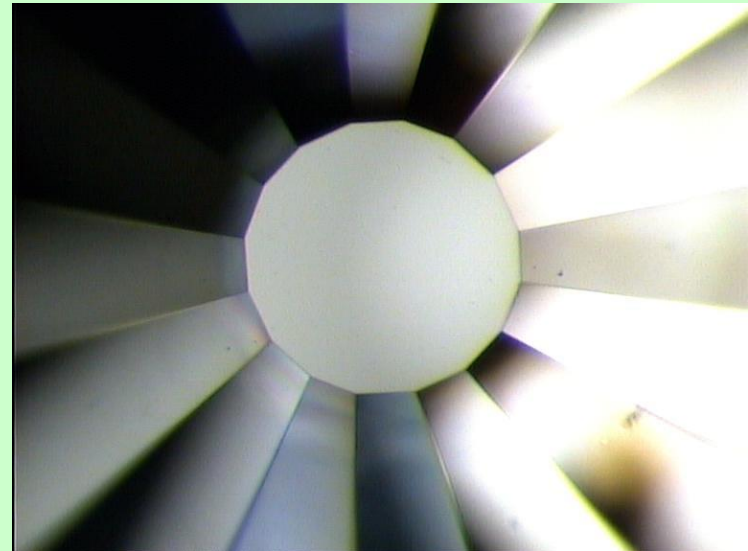
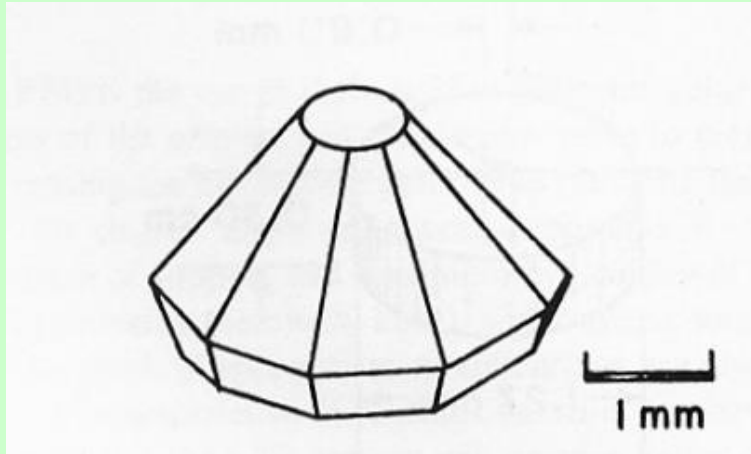
Alvin Van Valkenburg

The idea of an opposed diamond configuration for generating high pressure was developed by Weir, Lippincott, Van Valkenburg, and Bunting. *J. Res. Natl. Bur. Stand.* **63A**, 55, (1959), and Jamieson, Lawson and Nachtrieb. *Rev. Sci. Instrum.* 30, 1016, (1959).

High pressure can be achieved by applying a moderate force on a sample with a small area. In order to minimize deformation and failure of the anvils that apply the force, they must be made from a very hard and virtually incompressible material, such as diamond. Recently, 640 GPa was achieved by Dubrovinski, Dubrovinskaya, and Prakapenka, *Nature*, 3:1163, 2012.



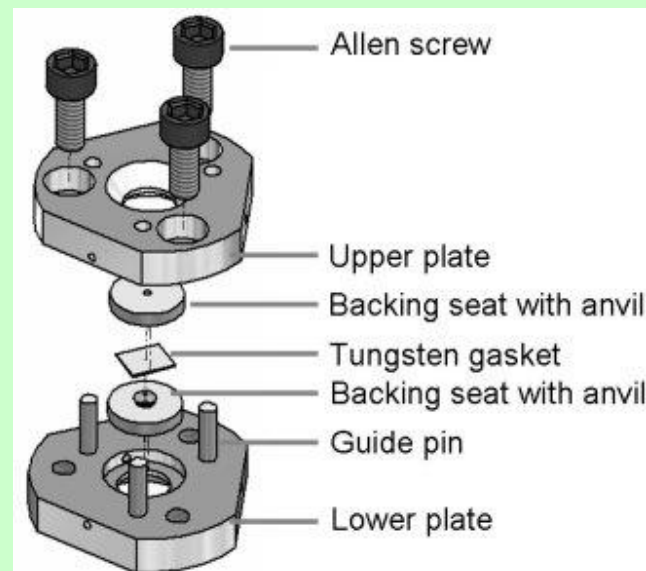
# Diamond Anvil Cell



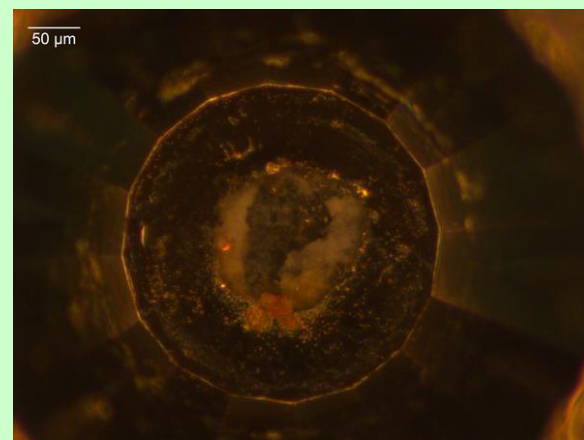
# Large Volume Press Apparatus and Diamond Anvil Cell



2000-ton hydraulic press with Walker module and DAC

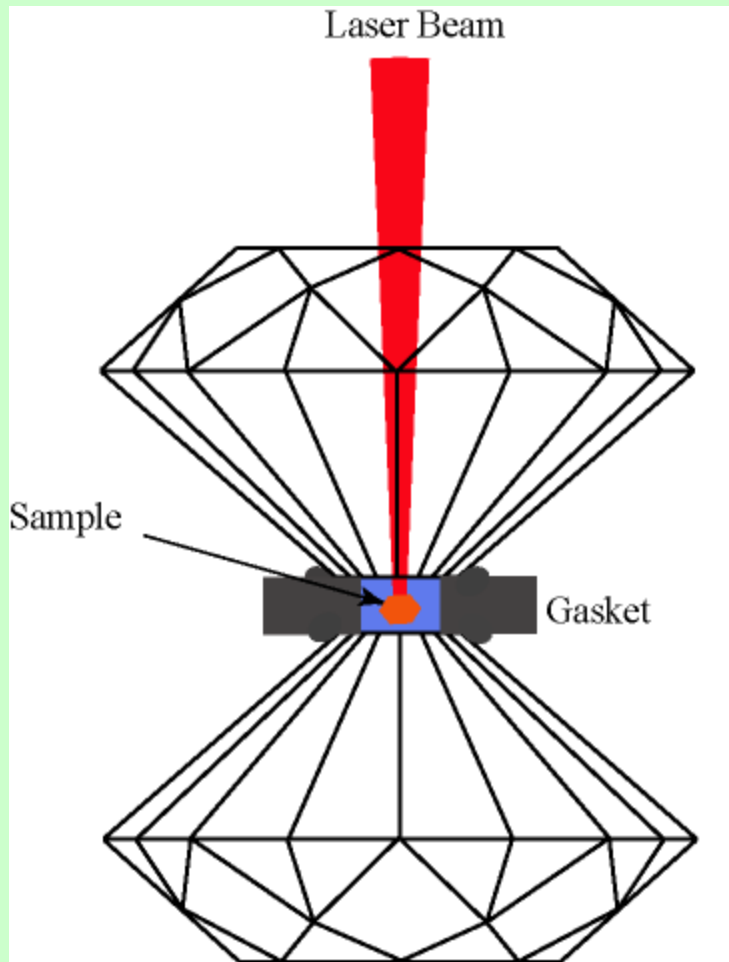


An exploded view of the diamond anvil cell used for high pressure X-ray diffraction experiments

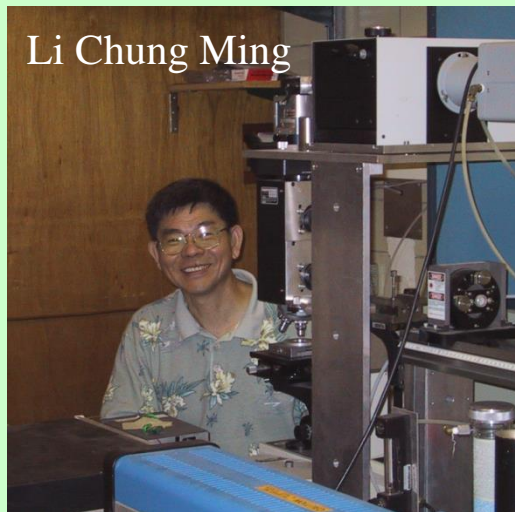


Optical image of BCx graphitic specimen after laser heating to 2200 K at 44 GPa.

# Development of Laser Heating in DAC

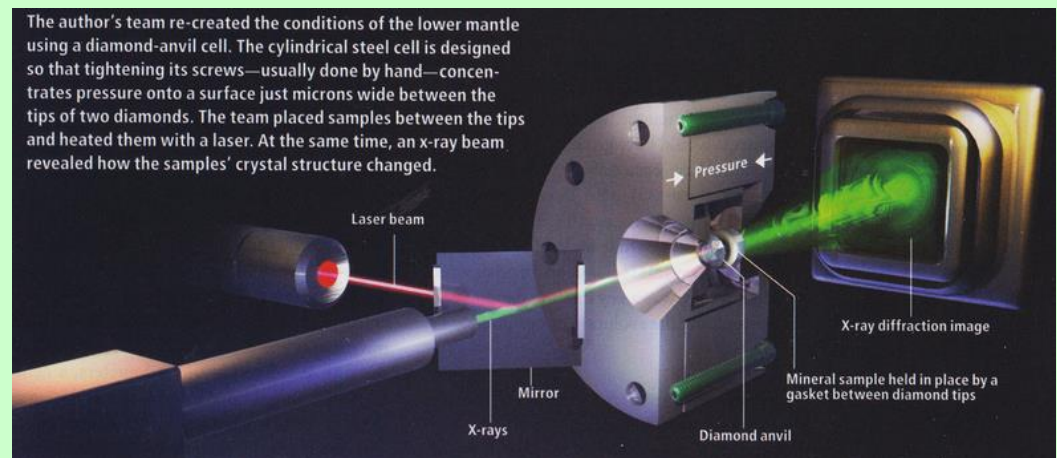


It simplified the sample assemblage in the DAC by heating a portion of the sample that is only tens of microns across and well isolated from the anvils.. Temperatures up to several thousand degrees and pressures up to megabars have been achieved.



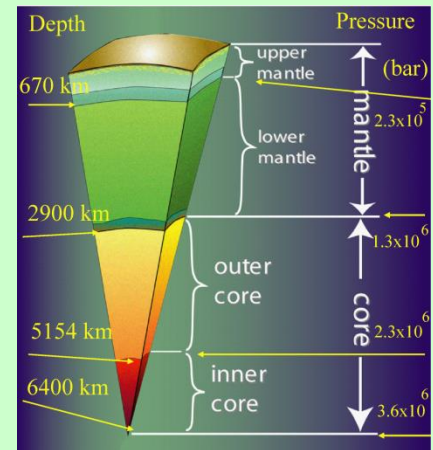
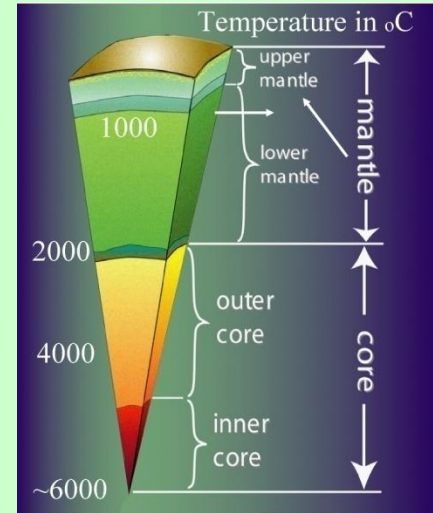
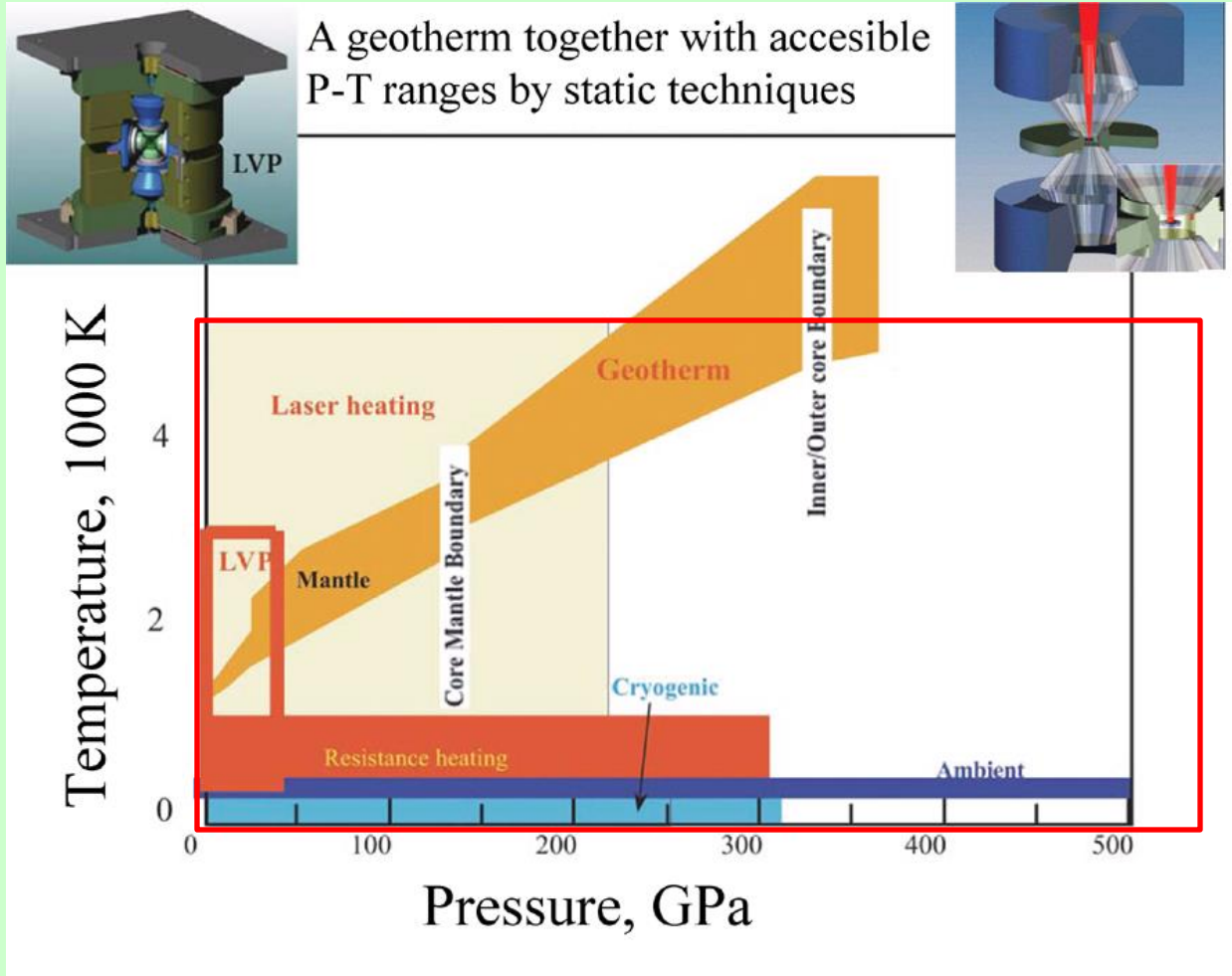
**Principles:** Laser heating is based on the principle of absorption of infrared laser light by the sample after the light has passed through one or both of the diamond anvils with only minor intensity loss.

**Post-perovskite** phase of  $\text{MgSiO}_3$  phase was discovered in 2004 using the laser-heated diamond anvil cell (125 GPa, 2500 K) by Murakami *et al.* (Science 2004)

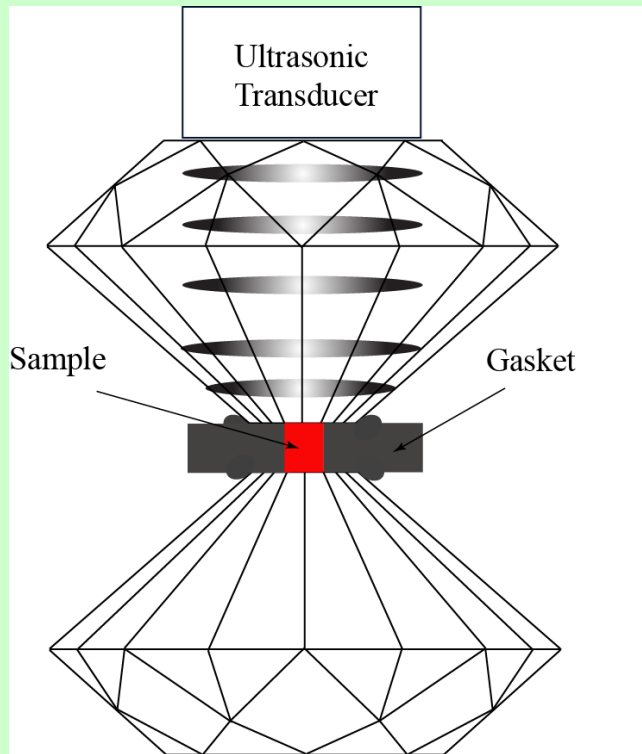


# Apparatus to Study the Interior of the Earth

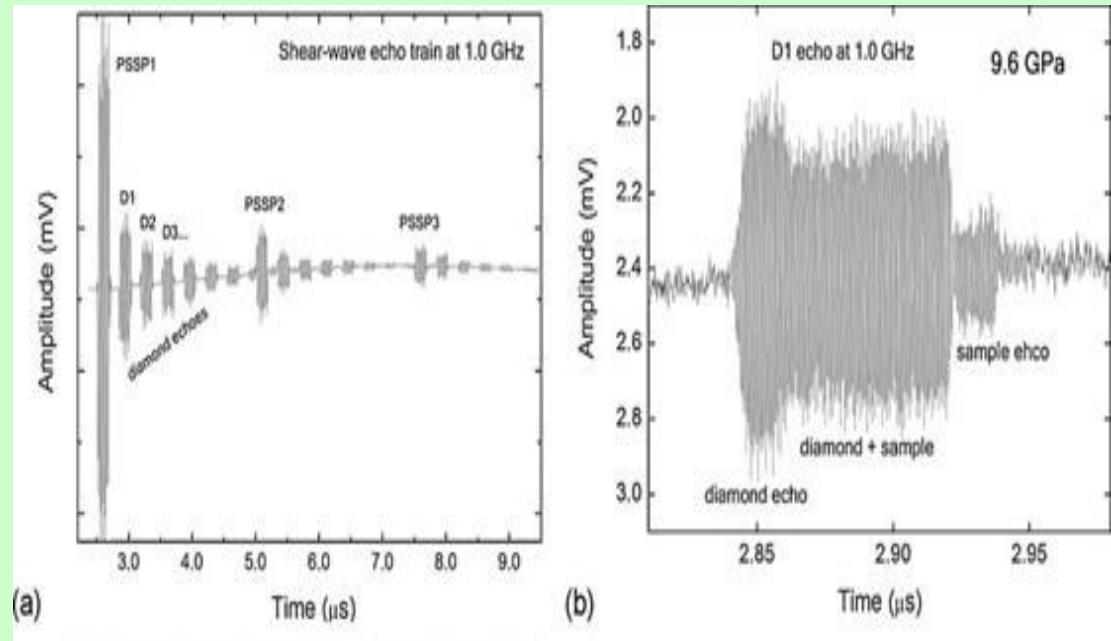
Pressure at the center of the: Earth = 300 GPa; Uranus = 600 GPa; Saturn = 1400 GPa; Jupiter = 2000 GPa



# Acoustical Wave Velocities in DAC by Ultrasonic Interferometry



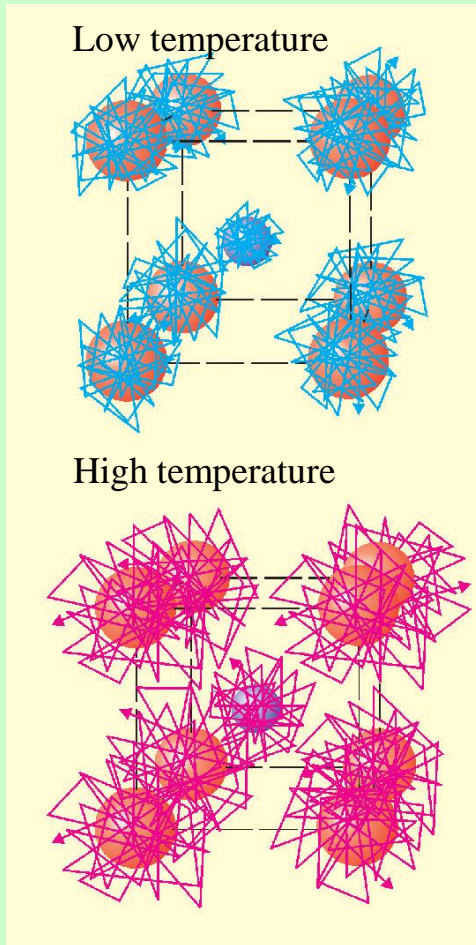
Schematic of acoustical wave propagation in DAC Ultrasonic Interferometry



Shear-wave interferometry data from a crystal of  $(\text{Mg}_{0.22}\text{Fe}_{0.78})\text{O}$  at 9.6 GPa in the diamond anvil cell. (a) Echo train at 1 GHz showing reflections internal to the buffer rod (labeled PSSP) and multiple S-wave echoes in the diamond (labeled D1, D2, etc.). (b) Expansion of the D1 echo, about 100 ns in duration, reveals the interference between the diamond and sample echoes. The amplitude is measured as a function of frequency at two positions, first before the sample echo arrives (diamond echo) and secondly where there is first-order interference between the diamond and sample. (Jacobsen, Reichman, *et al.*, *Advances in High-Pressure Techniques for Geophysical Applications*, Elsevier, Amsterdam, 2005).

# Sound Velocity Measurements in DAC: Brillouin scattering

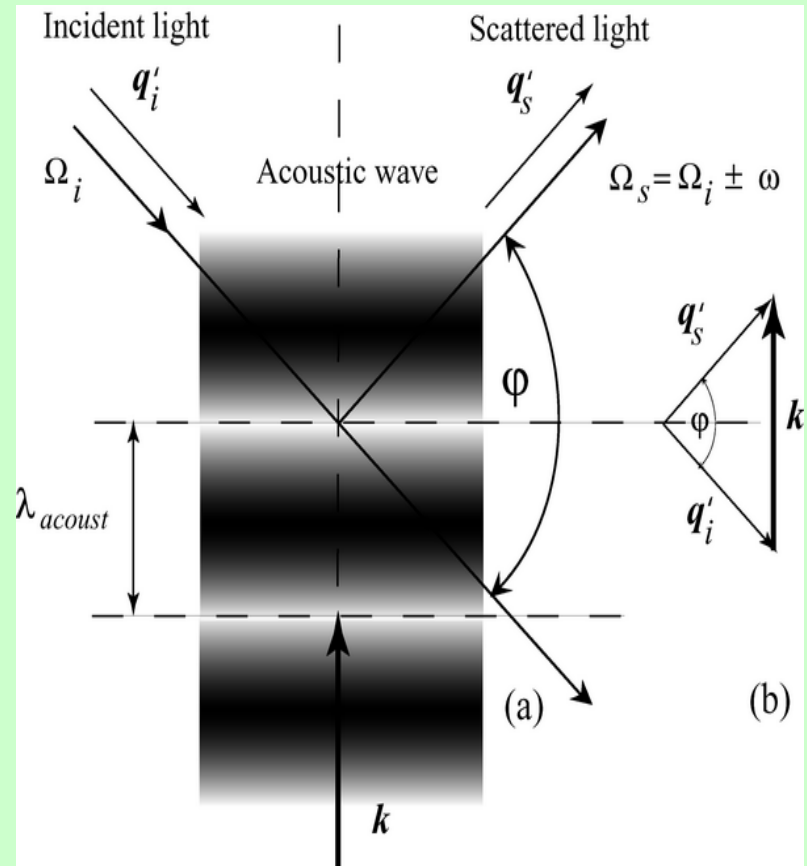
Definition: Brillouin scattering (BLS) is defined as inelastic scattering of light in a physical medium by thermally excited acoustical phonons.



Thermal vibrations of atoms

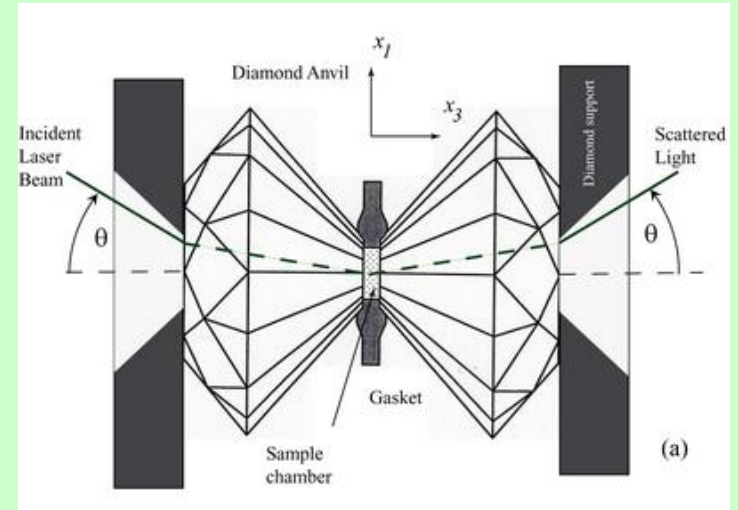
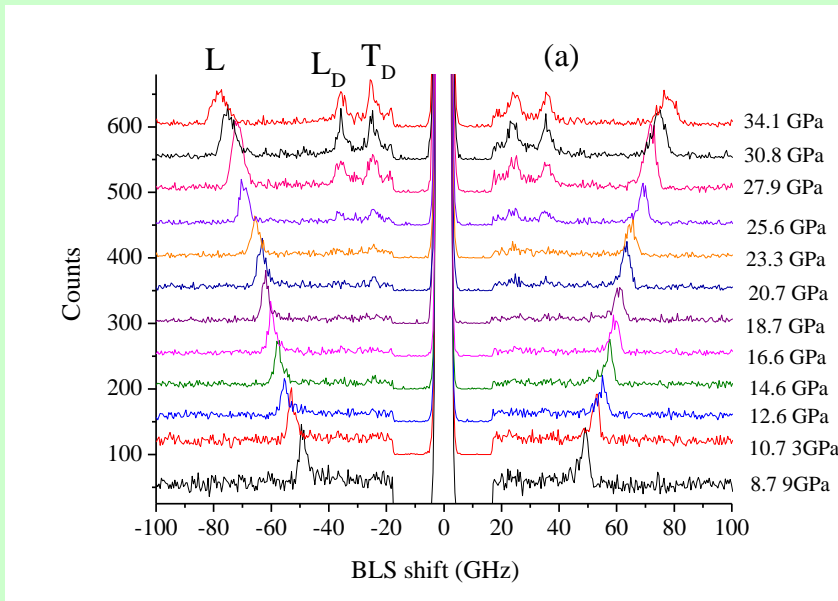
The moving grating scatters the incident light with a Doppler effect, giving scattered photons shifted frequencies  $\Delta f$ . The Brillouin spectrum gives the frequency shift ( $\Delta f$ ) of the thermal phonon, and its wavelength ( $d$  spacing). The grating space is equal to phonon wave length

$$V = \frac{\lambda_o \Delta f}{2n \sin\left(\frac{\varphi}{2}\right)}$$



Sketch of the light interaction with acoustic.

# Sound Velocity Measurements in DAC: Brillouin scattering



Arrangement for conducting BLS experiments in a DAC

Representative BLS spectra of  $g\text{-C}_3\text{N}_4$  collected inside a DAC: backscattering configuration.

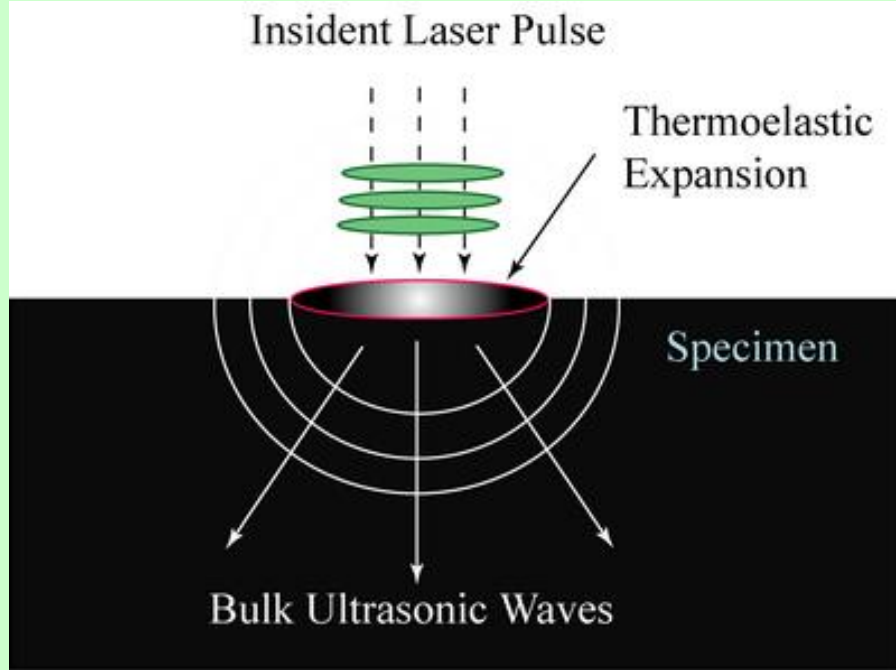
Then the velocity of the phonon  $V$  has the form

$$c_{acoust\_platelet} = \frac{\lambda_o \Delta f}{2 \sin \theta}$$

M. G. Beghi, A. G. Every, V. Prakapenka and P. V. Zinin. "Measurements of the Elastic Properties of Solids by Brillouin Spectroscopy", in T. Kundu ed., *Ultrasonic Nondestructive Evaluation: Engineering and Biological Material Characterization*. Taylor & Francis, N.Y., chapter 10, second edition, 540-612 (2012).



# Generation of Acoustical Waves by Laser



A schematic of the geometry of a *non-transparent* sample excited by a laser source

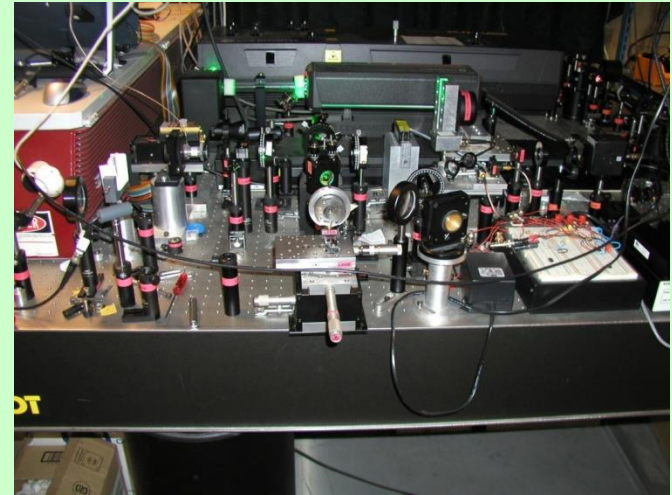
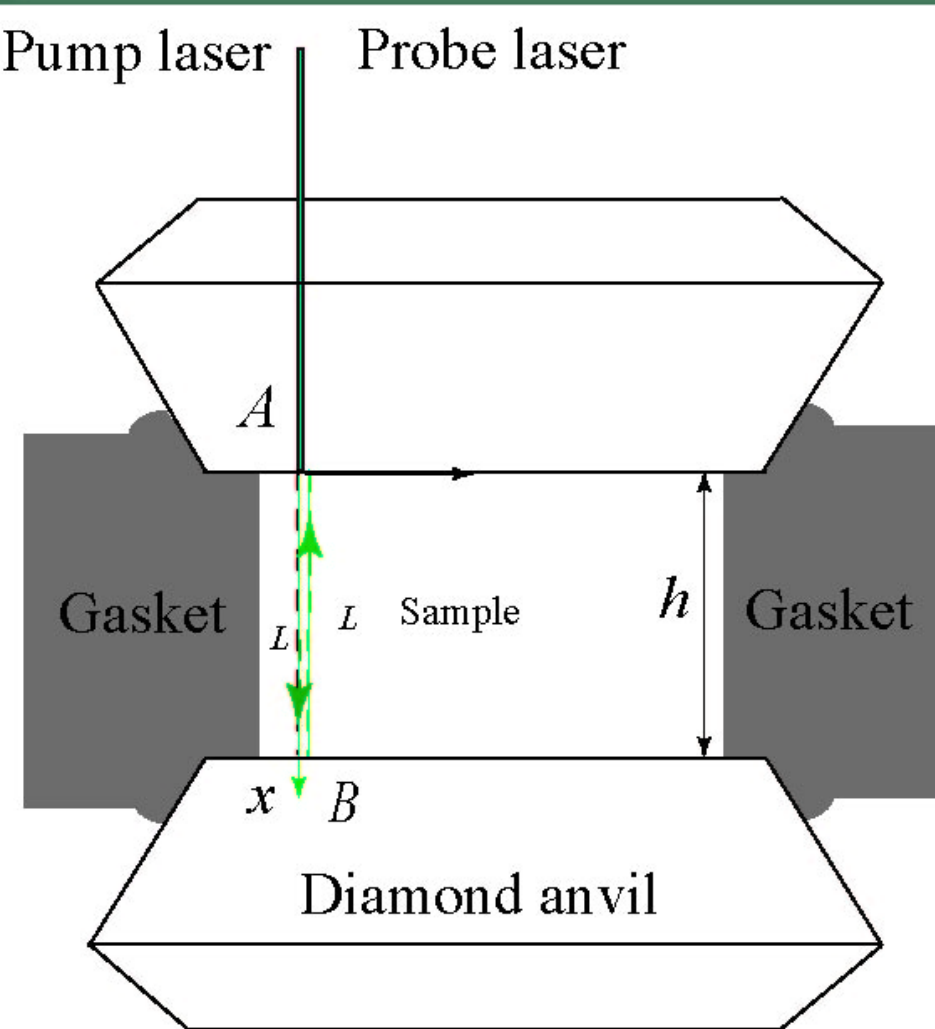
When an ultra-short laser pulse, known as the pump pulse, is focused onto an opaque surface, the optical absorption results in a thermal expansion that launches an elastic strain pulse. This strain pulse mainly consists of longitudinal acoustic waves that propagate directly into the bulk.

The stress  $p'$  producing in the medium is given by laser heating

$$p' = \rho_o c_o^2 \alpha_T \Delta T$$

where  $\Delta T$  is the temperature rise,  $\rho_o$  is the density of the medium,  $c_o$  is the sound velocity in the medium,  $\alpha_T$  is the linear thermal expansion coefficient, and  $\Delta T$  is the temperature change (Karabutov).

# Laser Ultrasonics (LU) in Diamond Anvil Cells (LU-DAC)

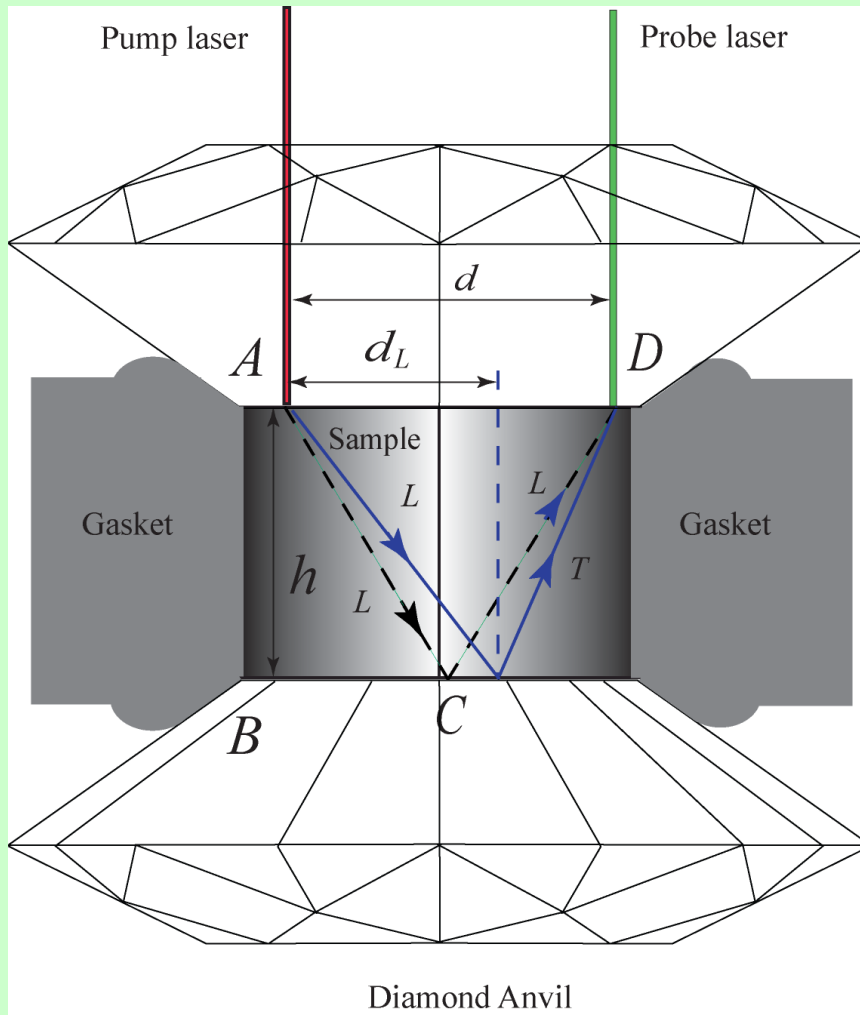


$$\tau = \frac{2h}{c_L}$$

$\tau$  is the time of flight (of sound pulse),  
 $c$  is the sound velocity and  $h$  is  
the sample thickness

Probe and pump lasers are on the same sides.

# Laser Ultrasonics (LU) in Diamond Anvil Cells (LU-DAC)



The time delay for the arrival of the  $LL$  and  $TT$  echoes  $\tau_{ss}$  is equal to

$$\tau_{\alpha\alpha}^2 = c_{\alpha}^2 d^2 + 4h^2$$

$$\alpha = L, T$$

if we introduce following variables,

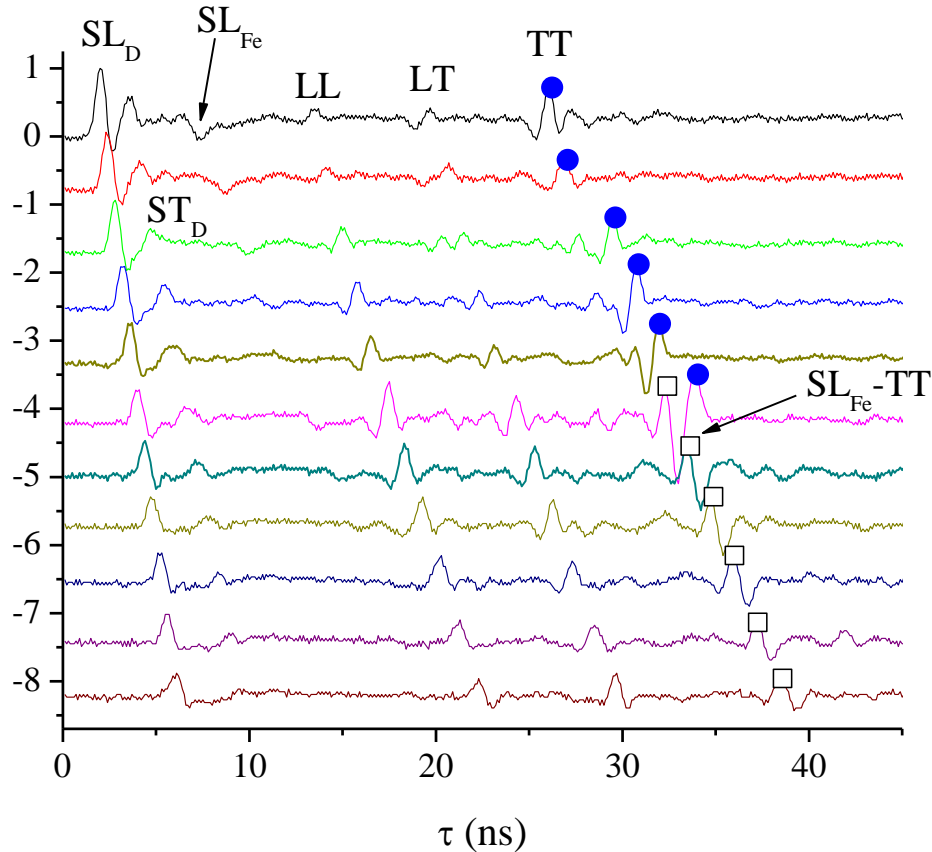
$$s = d^2, \tau = \tau_{\alpha\alpha},$$

then the equation above can be rewritten

$$s = c^2 \tau - 4h^2$$

LU-DAC, point-source - point-receiver technique: sound velocities can be determined from the linear fitting of the experimental data in  $(s, \tau)$  coordinates.

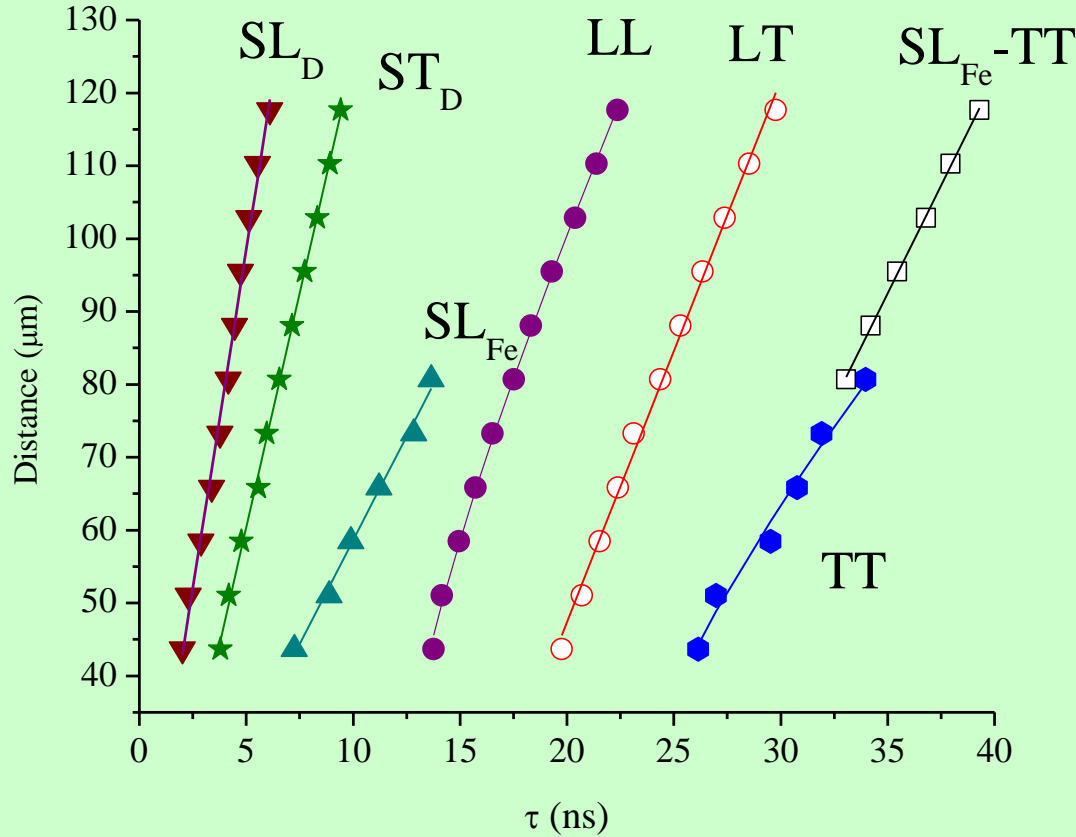
# Measurements of Longitudinal and Shear Wave Velocities in Iron by LU-DAC



Peaks  $P_1$  can be attributed to the arrival, with the time delay  $\tau_{LL}$  after the propagation in iron, of the  $LL$  wave that is excited as the longitudinal ( $L$ ) wave at the diamond/iron interface and is reflected by the iron/diamond interface as the longitudinal ( $L$ ) wave. Peak  $TT$  is attributed to arrival of the transverse-transverse ( $TT$ ) wave with time delay  $\tau_{TT}$ , and the  $P_2$  peak with time delay  $\tau_{LT} = \tau_{TL}$  is due to  $LT$  and  $TL$  acoustic mode conversion at the rear surface of the iron layer.

The signals measured at different distances  $d$ . The step of the scan is  $7.4 \mu\text{m}$ . The top signal was measured at  $d = 43.6 \mu\text{m}$ . Pressure was 10.9 GPa (N. Chigarev, P. Zinin, L.C. Ming, G Amulele, A. Bulou, V. Gusev., *Appl. Phys. Lett.*, **93**(18) 181905, 2008).

# Longitudinal and Shear Wave Velocities in Iron by LU-DAC



Fitting of the  $P_1$ ,  $P_2$  and  $P_3$  peaks at 22 GPa.

$$\tau_{LT} = \frac{\sqrt{d_L^2 + h^2}}{c_L} + \frac{\sqrt{(d - d_L)^2 + h^2}}{c_T}$$

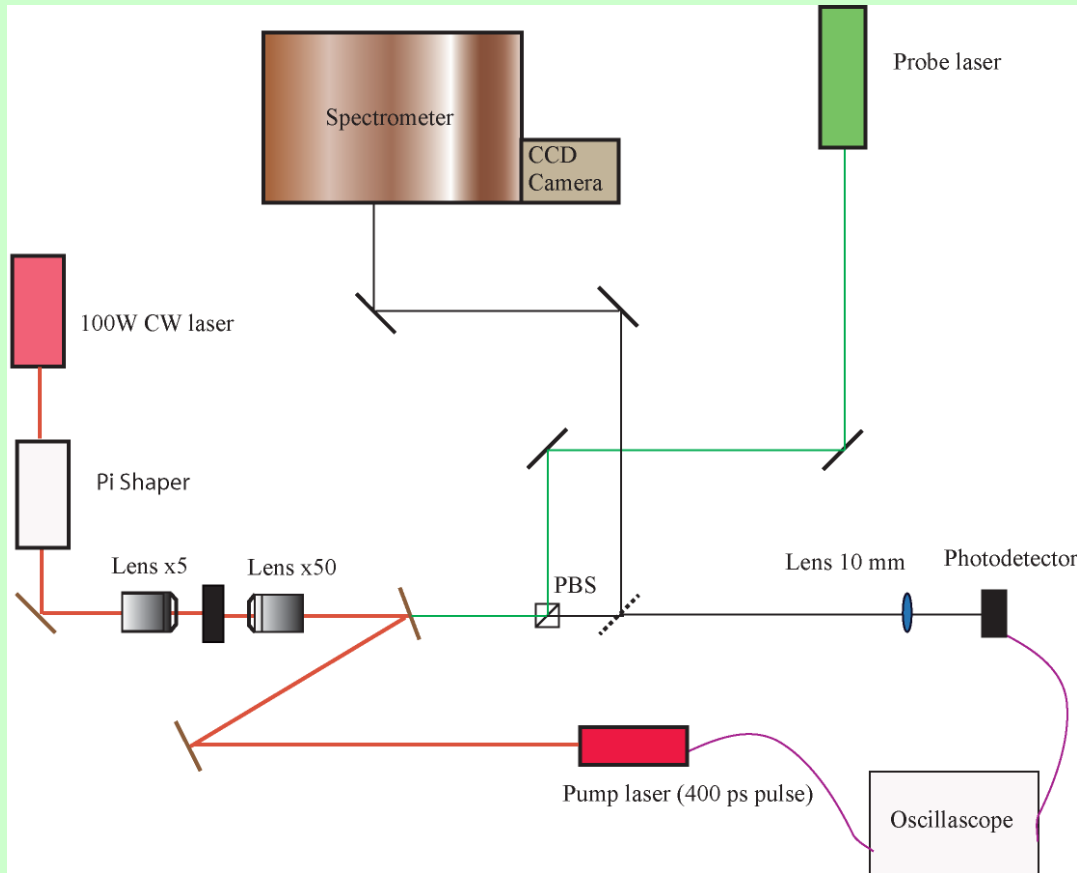
$$\frac{d_L}{c_L \sqrt{d_L^2 + h^2}} = \frac{d - d_L}{c_T \sqrt{(d - d_L)^2 + h^2}}$$

$$\delta^4 - 2\delta^3 + (1 + \xi^2)\delta^2 - 2\frac{\gamma^2}{(1 - q^2)}\delta + \frac{\gamma^2}{(1 - q^2)} = 0$$

where  $\delta = dL / d$ ,  $\xi = (h/d)$ ,  $\gamma = \tau LT c_L / d$ ,  $q = c_T / c_L$

Fitting of the  $SL_D$ ,  $ST_D$ ,  $SL_{Fe}$ , LL, LT/TL and  $SL_{Fe}$ -TT wave arrivals at 10.9 GPa. Thickness of the sample is taken from LL measurement to fit LT and TT peaks.

# Laser Ultrasonic-Laser Heating in Diamond anvil Cell (LU-LH-DAC) system



The system allows us to:

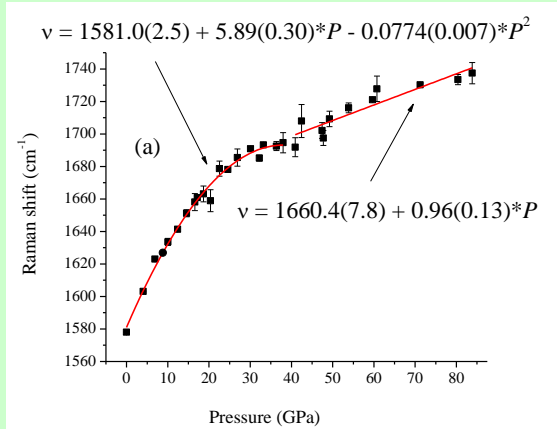
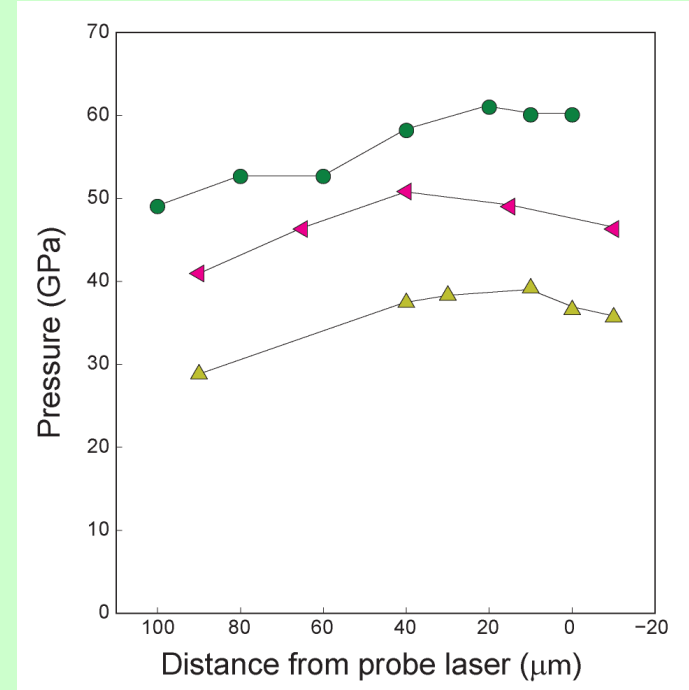
- (a) measure acoustical properties of materials under HPHT;
- (b) synthesize new phases under HPHT; and
- (c) measure Raman scattering under HPHT conditions for detection of phase transition.



A sketch of the LU-LH system.(K. Burgess et al., *Ultrasonics*, **54**, 963, 2014).

Control Panel of the LU-LH-DAC system

# Laser Ultrasonic-Laser Heating in Diamond anvil Cell (LU-LH-DAC) system



Upper image: Image of the combined LU-DAC and laser heating system at UH.

Pressure distribution inside DAC with iron, measured using Raman spectra of diamond

Center of the Raman G band of the graphite as a function of pressure.

# Temperature measurements

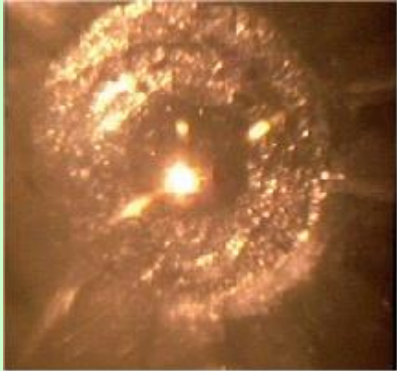
Usually temperature ( $T$ ) is calculated from the radiation ( $I$ ) emitted from a material heated by the laser using Planck's blackbody equation

$$I(\lambda) = \frac{\varepsilon c_1}{\lambda^5 \left[ \exp\left(\frac{c_2}{\lambda T}\right) - 1 \right]}$$

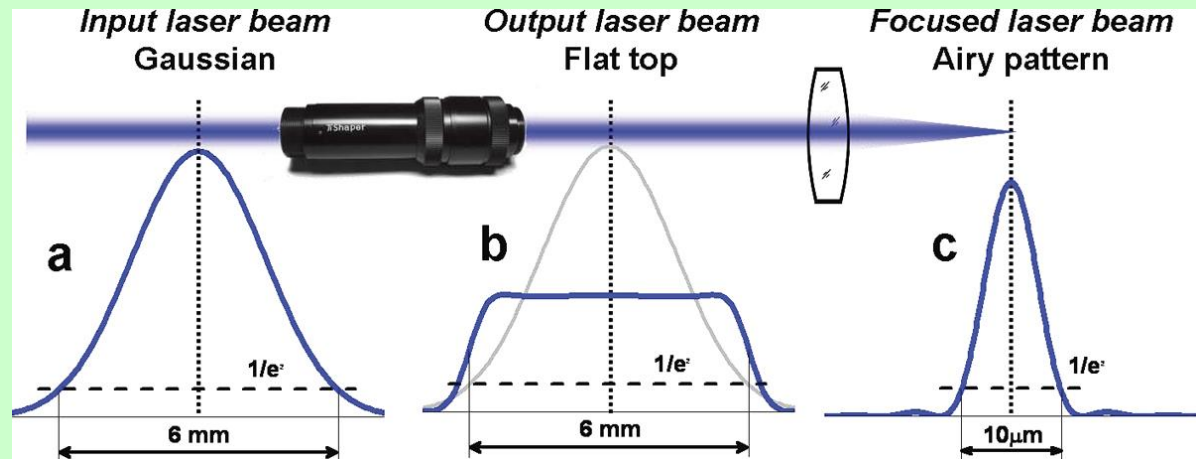
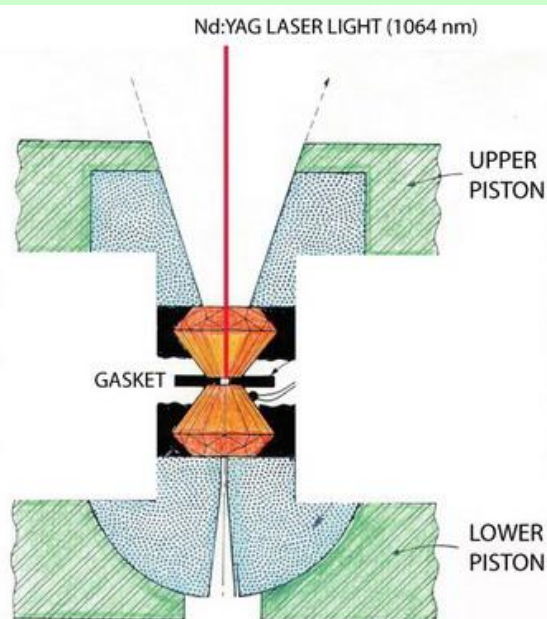
$$c_1 = 2\pi c^2,$$

$$c_2 = h^*c/k$$

$$= 0.01432 \text{ m}\cdot\text{K}.$$

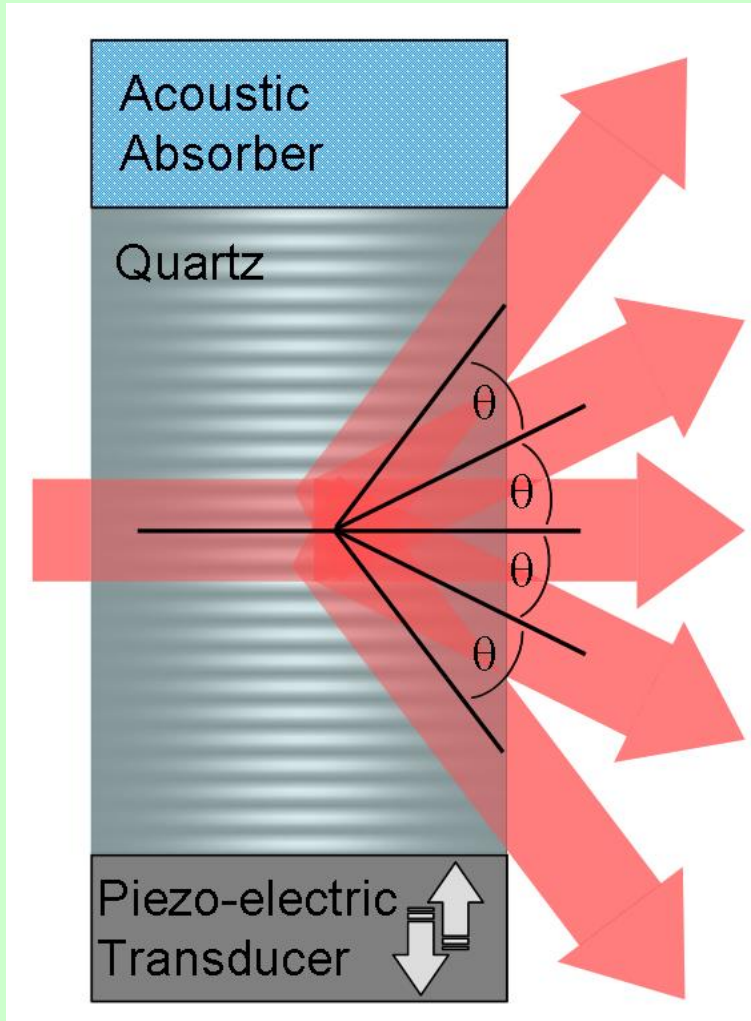


where  $I(x,y)$  and  $\varepsilon(x,y)$  are spectral intensity and emissivity at point  $x, y$ ,  $\lambda$  is wavelength,  $c_1$  and  $c_2$  are physical constants, and  $T$  is temperature.

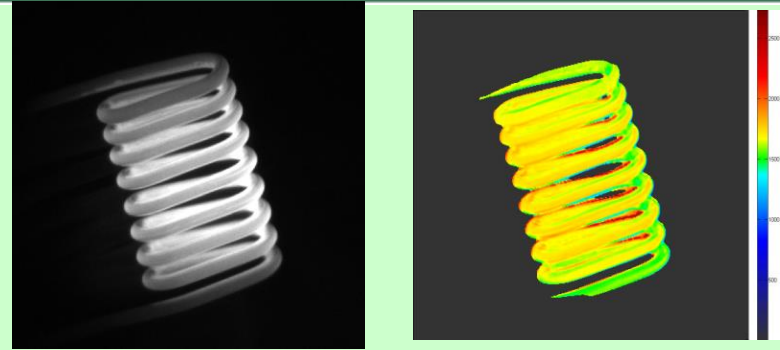


(Color online) Laser beam intensity profiles: a - Gaussian shape 6mm in diameter at an intensity level of  $1/e^2$ , b - flat top distribution at output of Pi-shaper, c - after focusing with 60mm focal length objective.

# Imaging system based on a tandem acousto-optical tunable filter for in-situ measurements of the high temperature distribution



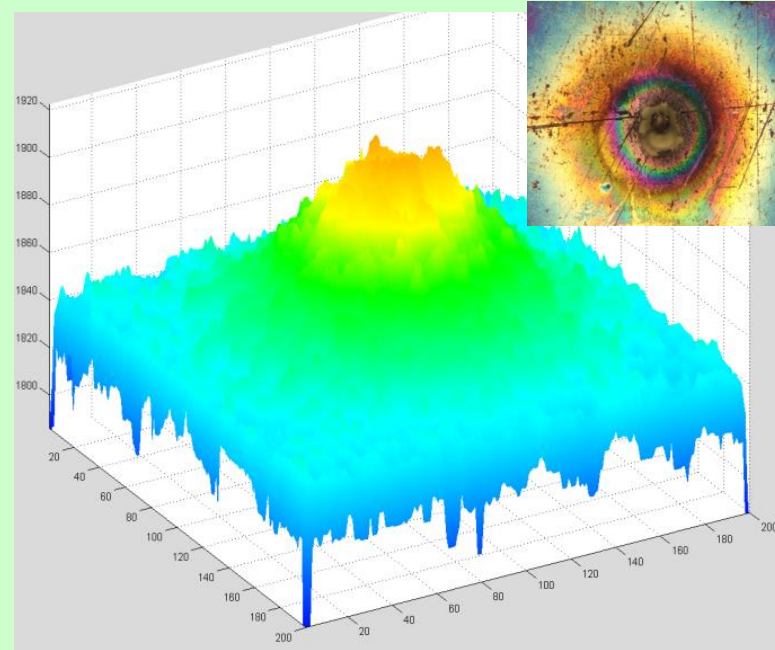
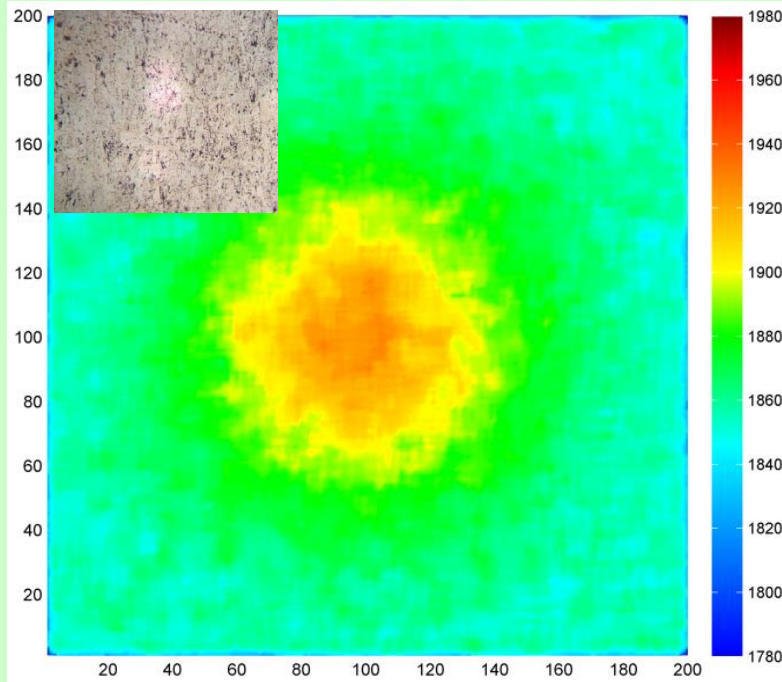
An acousto-optic filter



- (a) TAOTF spectroscopic image at  $\lambda = 800$  nm;  
(b) derived 2-D temperature distribution;  
(c) line scan of the temperature from point A to B;  
(d) line scan of the temperature from point C to D (Machikhin,, Zinin *et al. Opt. Lett.* 45, 2016).

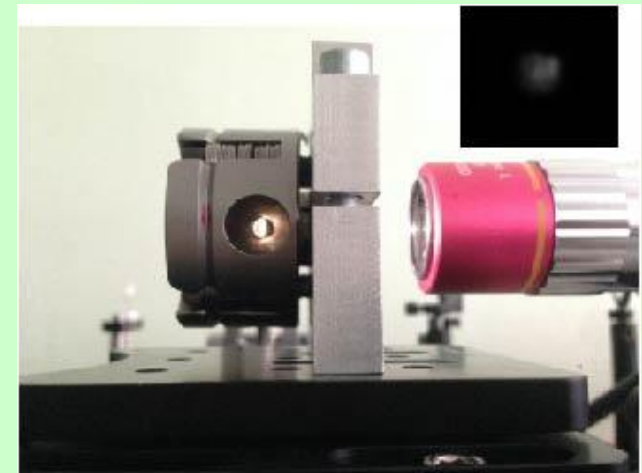
The principle behind the operation of acousto-optic filters is based on the wavelength of the diffracted light being dependent on the acoustic frequency. By tuning the frequency of the acoustic wave, the desired wavelength of the optical wave can be diffracted acousto-optically.

# Imaging system based on a tandem acousto-optical tunable filter for in-situ measurements of the high temperature distribution

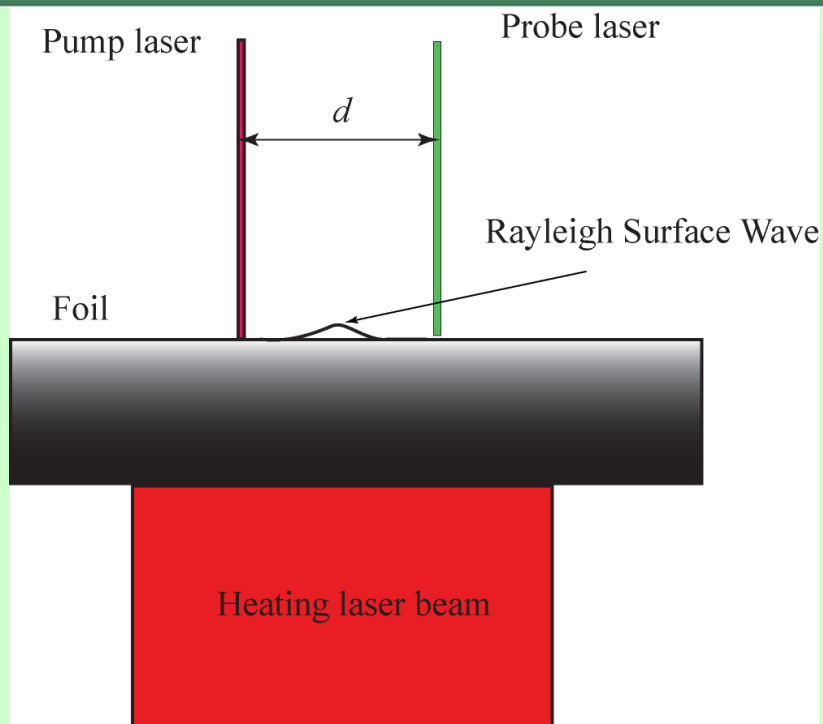


Temperature distribution on tungsten plate under laser heating (Machikhin *et al.*, Приборы и техника эксперимента, 2016, in press.)

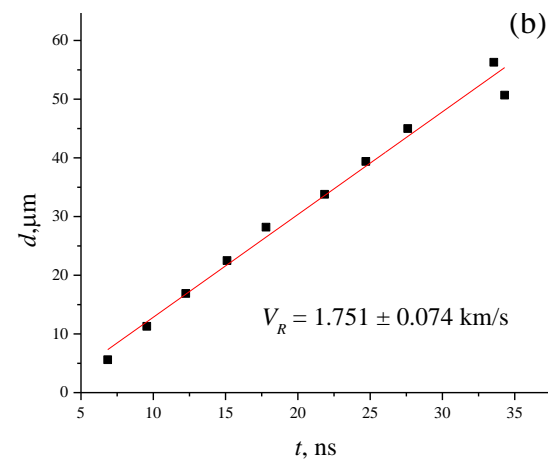
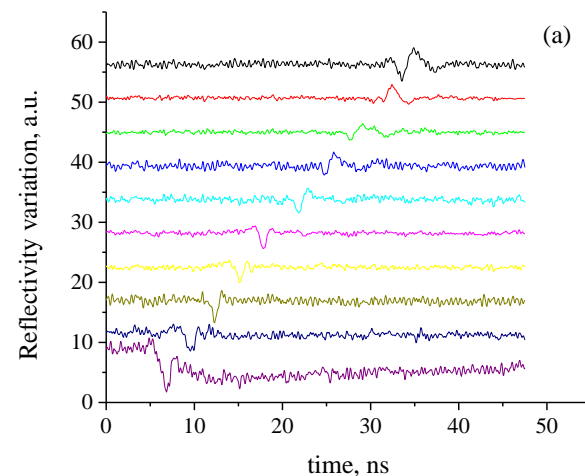
Laser heating of the g-C<sub>3</sub>N<sub>4</sub> specimen. Insert is the spectroscopic image taken at 1020 nm.



# Laser Ultrasonic-Laser Heating in Diamond anvil Cell (LU-LH-DAC) system

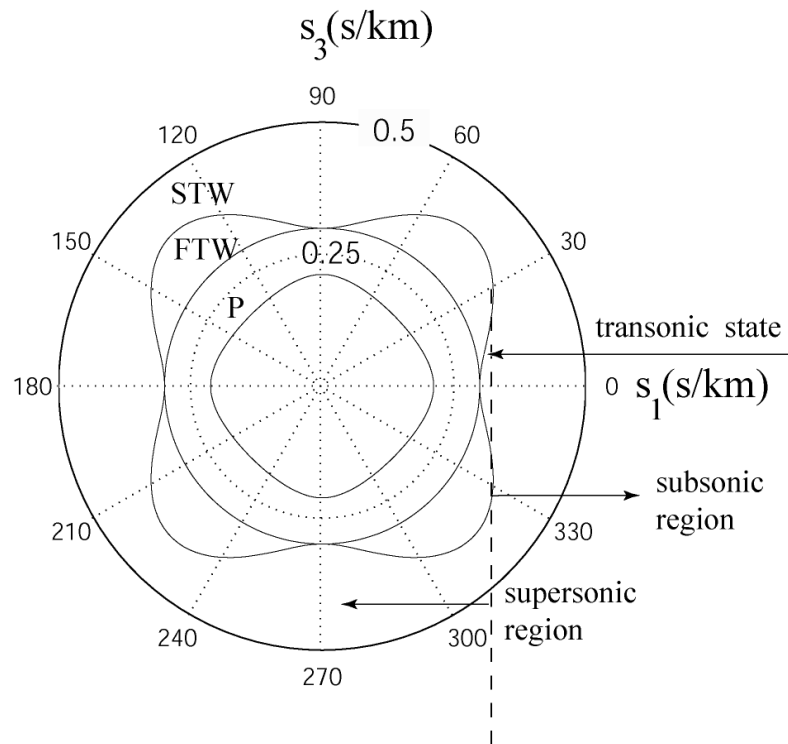


A sketch of the surface acoustic wave excitation and detection in the laser heated foil (K. Burgess et al., *Ultrasonics*, **54**, 963, 2014).

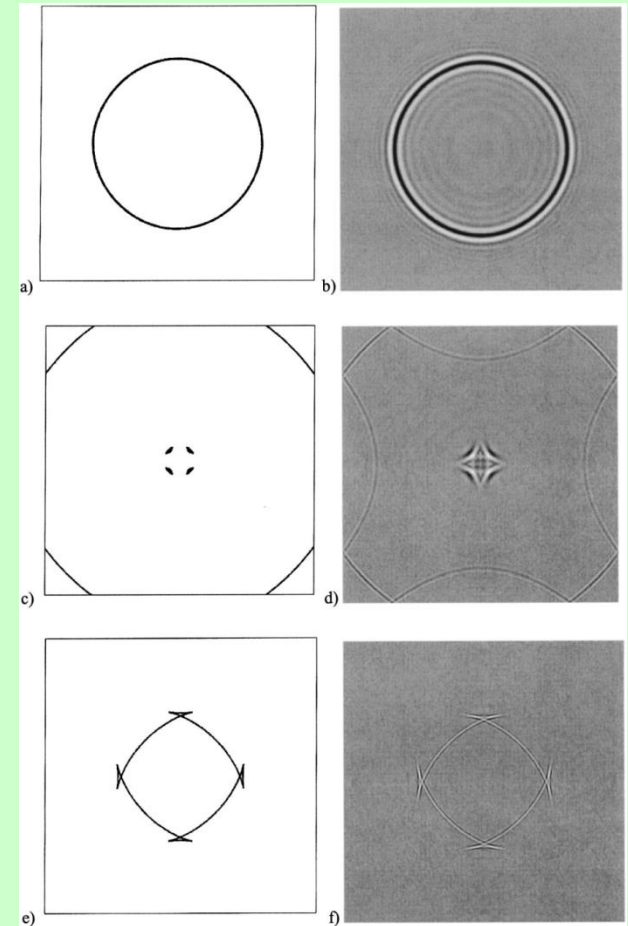


(a) Raw data for the transient reflectivity change at different distances  $d$  at 1100 K. The scales are common for all the curves, which are shifted vertically for clarity. The step of the scan is  $5.6 \mu\text{m}$ . (b) Arrival time of the Rayleigh wave in platinum at 1100 K as a function of position of the probe laser  $d$ .

# Phonon Focusing in Crystals

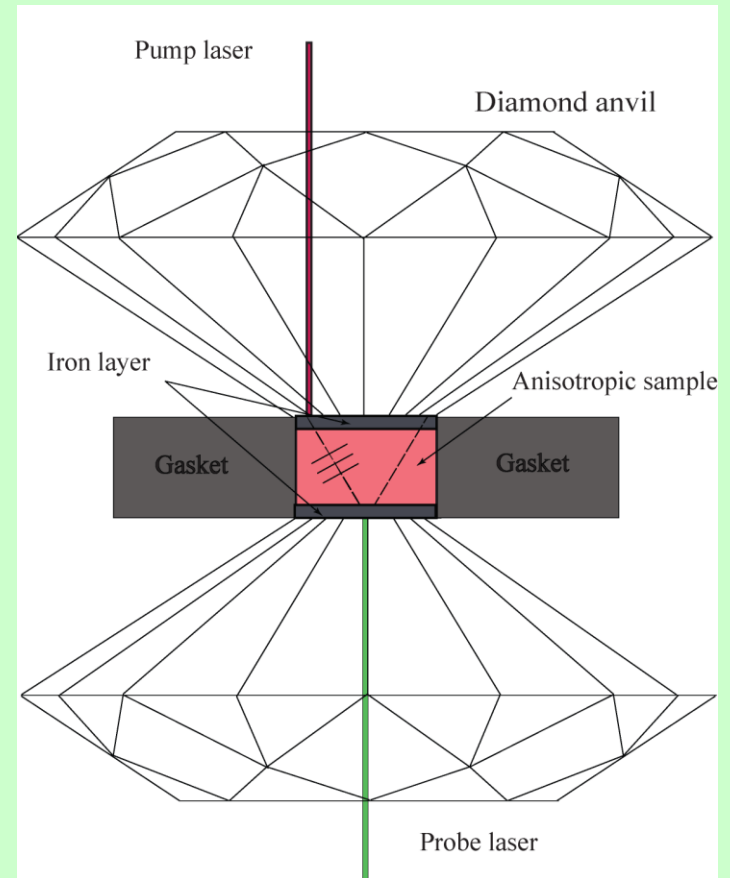
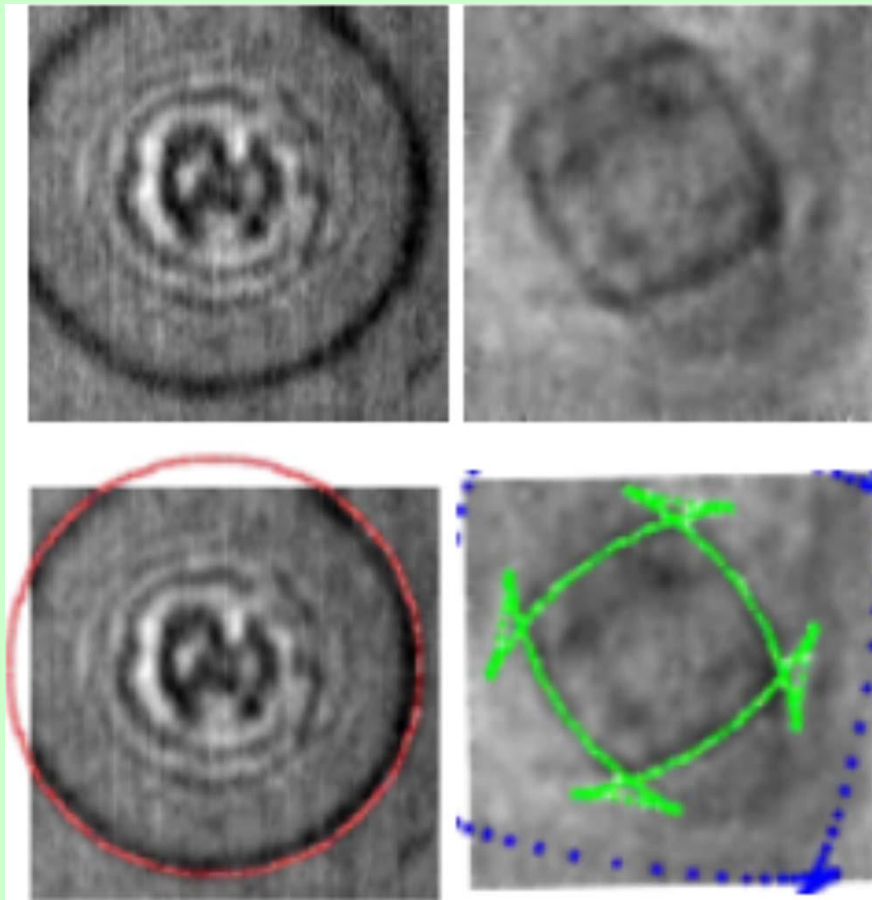


The slowness curve of silicon for the (001) plane. The dashed line corresponds the transonic state. The solid curves correspond the slowness curves for longitudinal P, FT and ST bulk waves.



Numerical simulation of a short-pulse transient signal in a (001)-oriented Si crystal. (From Pluta, Every, *PRB*, 2003).

# Future work: Phonon Focusing in Crystals for Elastic Moduli Determination



Top: experimental phonon imaging patterns in the 100 plane of silicon at 7.75 GPa at two different pump-probe delays. Bottom: same as top with superimposed calculation curves for longitudinal, fast, and slow transversal group velocities red, blue, and green dashed lines, respectively using  $C_{11} = 196.9$  GPa,  $C_{12} = 104$  GPa, and  $C_{44} = 80$  GPa (Decremps *et al.*, Phys. Rev. B **82**, 104119 2010).

# Techniques to Study the Elasticity of Materials under HPHT

- 1) Brillouin scattering works for measuring of elastic properties of *transparent* materials.
- 2) Impulsive Stimulated Light Scattering (ISLS) does not allow *simultaneous* determination of shear and longitudinal velocities [J.C. Crowhurst et al *Phys. Rev. B* **64** 100103 (2001)].
- 3) Inelastic X-ray scattering (IXS) from phonons is analogous to Brillouin scattering, but with X-rays instead of visible light. [G. Fiquet et al *Science* **291**, 468 (2001)] ( $v_L$  *Iron* at 20-110 GPa)
- 4) Laser was applied for the first time to excite longitudinal acoustic waves in DAC. [M. Villagran-Muniz et al, *Rev. Sci. Instrum.* **74**, 732 (2003)].
- 5). Picosecond ultrasonics uses pump-probe technique with 100 fs laser to excite and detect the longitudinal acoustic waves. [F. Decremps et al *Phys. Rev. Lett.* **100**, 035502 (2008)].
- 5) Laser ultrasonics in diamond anvil cell (LU-DAC) technique uses 750 ps laser pulses to excite the sound and CW to probe [N. Chigarev et al *Appl. Phys. Lett.* **93**, 181905 (2008)].

